

Most sperm undergo acrosomal exocytosis in the upper oviductal isthmus

¹Florenza A. La Spina; ¹Ana Romarowski; ¹Lis C. Puga Molina; ¹Tomas L. Falzone;
¹Alejandra M. Vitale; ²Noritaka Hirohashi; ¹Mariano G. Buffone*.

¹*Instituto de Biología y Medicina Experimental (IBYME), Consejo Nacional de Investigaciones Científicas y Técnicas (CONICET), Buenos Aires, Argentina.* ²*Oki Marine Biological Station, Education and Research Center for Biological Resources, Shimane University, Japan.*

Grant support: National Institutes of Health (NIH, RO1TW008662), *Agencia Nacional de Promoción Científica y Tecnológica* (PICT 2013-1175).

Running title: Mouse sperm acrosomal exocytosis in vivo

Keywords: Sperm; acrosomal exocytosis; oviduct; fertilization; acrosome

***Corresponding authors:**

Mariano G. Buffone Ph.D.
Instituto de Biología y Medicina Experimental
Vuelta de Obligado 2490 (1428)
Buenos Aires, Argentina
Tel. (+5411)4783-2869
Fax. (+5411)47862564
mgbuffone@ibyme.conicet.gov.ar

Abstract

Mammalian sperm are not able to fertilize oocytes immediately after ejaculation; they must first undergo a complex process called capacitation in the female reproductive tract or *in vitro*. These changes include the development of hyperactivated motility and the ability to undergo acrosomal exocytosis (AE) in response to specific stimuli. Recent evidence demonstrated that most fertilizing sperm undergo acrosomal exocytosis before binding to the Zona Pellucida (ZP) of the eggs. However, it is still unknown the site where fertilizing mouse sperm initiate AE and what stimuli trigger it. Therefore, the aim of this study was to determine the physiological site of AE by using EGFP sperm in a combination of *in vitro* and *ex-vivo* approaches. In the *ex-vivo* experiments, it was evaluated the occurrence of AE within the female reproductive tract, in the physiological context where this process occurs. Using live imaging of transgenic EGFP sperm during *in vitro* fertilization with COCs it was observed that AE rarely occurred while sperm were passing through the cumulus *in vitro*. Most of sperm that migrated through the UTJ and formed the sperm reservoir in the isthmus are acrosome intact. The analysis of the upper segments of the oviduct revealed that a significant number of sperm underwent AE in the upper isthmus. In the ampulla, very few sperm were detected and only 5% of the sperm in this region were acrosome intact. These results support previous observation that sperm does not initiate AE in the vicinity or upon contact to the ZP and strongly suggest that most of the sperm may initiate the physiological AE in the upper segments of the oviductal isthmus.

Introduction

Mammalian spermatozoa are not able to fertilize oocytes immediately after ejaculation; they must first undergo a complex process called capacitation in the female reproductive tract or *in vitro* (Austin, 1951; Chang, 1951; Visconti, 2009). These changes include the development of hyperactivated motility and the ability to undergo acrosomal exocytosis (AE) in response to specific stimuli (Buffone et al., 2008, 2012; Suarez, 2008). AE is essential for fertilization. Mice and men that produce sperm lacking acrosomes are sterile (Dam et al., 2007; Kang-Decker et al., 2001; Lin et al., 2007). The occurrence of AE allows Izumo1, a protein that is essential for sperm-egg fusion, to relocalize to the equatorial region of mouse sperm head (Satouh et al., 2012) by an actin-dependent mechanism (Sosnik et al., 2009). Although AE shares similarities with exocytotic secretory mechanisms in other cells, it is considered to be a special type of controlled secretion (Buffone et al., 2014; Mayorga et al., 2007).

Not long ago, it was broadly accepted that sperm undergo AE upon interaction with the egg's zona pellucida (ZP), and many of the advances in our knowledge of this process were derived from *in vitro* studies using solubilized ZP (Cherr et al., 1986; Florman and Storey, 1982; Storey et al., 1984). However, recent evidence using transgenic mice that produce sperm which carry enhanced green fluorescent protein (EGFP) in the acrosome, suggest that sperm binding to the ZP is not sufficient to induce AE (Baibakov et al., 2007). This observation was later supported by real-time imaging of *in vitro* fertilization, which showed that most fertilizing sperm undergo AE before binding to the ZP (Jin et al., 2011). In fact, in that study, most acrosome-intact sperm were seen to move away from the ZP without entering it. A subsequent study demonstrated that acrosome-reacted sperm recovered from the perivitelline space of oviductal CD9^(-/-) oocytes are able to fertilize other cumulus enclosed oocytes *in vitro* (Inoue et al., 2011). This was also demonstrated in earlier studies using rabbit sperm (Kuzan et al., 1984). Thus, the initiation of sperm AE on

the ZP seems to be the exception, rather than the rule (Yanagimachi, 2011). This evidence strongly suggests that ZP may not be the primary physiological inducer of the acrosome reaction and at least partially, this controversy may have been originated by the fact that the effect of ZP on AE is strong when these proteins are solubilized but it is minimal or nonexistent when the ZP proteins are assembled in the real three-dimensional structure. However, Jin and associates did not identify the site where fertilizing mouse spermatozoa initiated AE and what stimuli trigger it (Jin et al., 2011). These are key events that remain to be determined.

While the ZP's role in triggering sperm AE needs major reconsiderations, progesterone has remained another favorable candidate for the AE inducer. Progesterone, a major secretory product from the cumulus cells surrounding the ovulated oocytes, has been long known to stimulate or prime AE (Osman et al., 1989; Roldan et al., 1994). Progesterone produces an increase in intracellular calcium that is essential for exocytosis to occur but the identity of its receptor in mammalian sperm has not been elucidated. These findings further support the possibility that AE can occur before sperm reach the ZP. In addition, the effects of Progesterone have also been implicated in other sperm functions such as chemotaxis, sperm motility and capacitation (Oren-Benaroya et al., 2008). In humans, it was recently demonstrated that progesterone can modulate the activation of CatSper channels which are essential for the development of hyperactivated motility (Ren et al., 2001).

The recent studies of AE were made possible by the development of double transgenic male mice [BDF1-Tg (CAG-mtDsRed2, Acr-EGFP) RBGS0020sb], which produce sperm that express EGFP green fluorescence in the acrosome and Ds-Red2 red fluorescence in the mitochondria of the flagellar midpiece (Hasuwa et al., 2010). This transgenic mouse has enabled investigators to examine the status of the acrosome in live sperm as they pass through cumulus-enclosed oocytes to fertilize them in vitro (Jin et al., 2011). However,

these mice also offer the opportunity to monitor the status of the acrosome in live, motile sperm swimming within the oviduct. Therefore, the aim of this study is to determine the physiological site of AE by using EGFP sperm in a combination of in vitro and ex-vivo approaches. We aimed to determine: i) the occurrence of AE while sperm are traveling through the cumulus cells matrix; ii) the occurrence of AE within the female reproductive tract, in the physiological context where this process occurs.

Materials and Methods

Animals

Mice were maintained at 23°C with a 12 h light:12 h dark cycle. Double-gene knockin males [BDF1-Tg (*CAG-mtDsRed2*, *Acr-EGFP*) RBGS0020sb], expressing EGFP in the acrosome and Ds-Red2 in flagellar midpiece mitochondria, were mated with 8-week old superovulated F1 females (C57BL/6JxBalBc) in order to detect and localize sperm within the oviduct. Superovulation was induced using pregnant mare serum gonadotropin (5IU, PMSG; Calbiochem) at 6:30 PM, followed 48 h later by human chorionic gonadotropin (5 IU, hCG; Calbiochem). Females were placed with males at 6:20 AM the following morning, and mating was allowed until 7:00 AM. The end of the mating period was considered as t=0. Mice were sacrificed by CO₂ asphyxiation and oviducts were collected 1.5 h and 4 h after the end of the mating period. Animal experimental procedures were reviewed and approved by the Ethical Committee of IBYME, Experiments were performed in strict accordance with the Guide for Care and Use of Laboratory Animals approved by the National Institutes of Health (NIH).

In addition to hormonal stimulation of superovulation, some [B6D2F1-Tg (*CAG/su9-DsRed2*, *Acr3-EGFP*) RBGS0020sb] males were mated with females undergoing natural estrous cycles. Visual assessment of cycle stage was used to select (C57BL/6JxBalBc) F1

females (Gates et al. 1973), which were then caged with males at 6:00 AM for 30 min. Mating was considered to have occurred if a vaginal plug was found afterward.

Oviduct preparation and imaging

The uterine horn was tied off and dissected out together with the oviduct and the ovary. Oviducts were gently washed in Whitten's medium (100 mM NaCl, 4.4 mM KCl, 1.3 mM CaCl₂, 1.2 mM MgSO₄, 1.2 mM KH₂PO₄, 20 mM sodium lactate, 5.4 mM glucose, 0.8 mM sodium pyruvate and 20 mM HEPES, pH 7.4) to remove sperm attached to the outside wall, mounted on slides and covered with coverslips. The coverslips were held up with silicon grease. To evaluate the migration of sperm through the female reproductive tract, oviducts were imaged using an inverted epifluorescence microscope (TE-2000U, Nikon) connected to a CoolSNAPHQ-cooled CCD camera (Roper Scientific) and driven by MetaMorph 7.0 (Universal Imaging Corporation). A microscope stage chamber (Harvard Apparatus) was used to maintain a humid atmosphere of 5% CO₂ in air and a heated stage was used to maintain the temperature at 37°C. Sperm were observed using a 20X objective and confocal microscopy (Nikon C1 Eclipse 800) (ZSTACK). The behaviors of sperm within each region of the oviduct [utero-tubal junction (UTJ), lower isthmus (LI), middle isthmus (MI), upper isthmus (UI) and ampulla (AMP)] were recorded and the number of sperm were counted manually using Image J (National Institutes of Health).

Analysis of sperm distribution in the oviduct using frozen sections

Oviducts of mated females were fixed with 4% paraformaldehyde in PBS and processed for cryosectioning (20 µm sections). The sections were stained with 0.001% Hoechst 33342 in PBS. Total numbers of sperm and the numbers of acrosome-reacted sperm (DsRed2-positive and EGFP-negative) in the oviduct lumen were counted in each of

region. ImageJ was used to keep track of the sperm counted in each histological section, such that no sperm that spanned more than one section were counted more than once.

Quantification of the percentage of fertilized oocytes post mating

Wild type female mice were superovulated following intraperitoneal injections of (PMSG) and human chorionic gonadotropin (hCG) at 48-h intervals and mated with transgenic males as described previously. Ovulated egg masses were recovered at 1.5 h, 4 h and 7 h after coitus in KSOM medium (95 mM NaCl, 2.5 mM KCl, 0.2 mM MgSO₄, 0.2 mM glucose, 10 mM sodium lactate, 25 mM NaHCO₃, 0.2 mM sodium pyruvate, 1.71 mM CaCl₂, 1 mM glutamine, 0.1 mM EDTA, 1 mg/ml BSA) and cultured for 24 h. Fertilization was confirmed by assessing the numbers of two-cell embryos.

Sperm capacitation

In vitro capacitation was performed as previously described (Jin et al., 2011). Briefly, spermatozoa from the cauda epididymidis of [B6D2F1-Tg (CAG/su9-DsRed2, Acr3-EGFP) RBGS002Osb] males were induced to capacitate by suspending them in a 100- μ L droplet of human tubal fluid (HTF)-BSA medium at \sim 105 cells/mL and then incubating them for 1–3 h at 37 °C under an atmosphere of 5% CO₂ and 95% air. Insemination was performed by placing about 1 μ L of capacitated sperm suspension (about 2,000 sperm) at the edge of a coverslip overlaying a slightly compressed cumulus–oocyte complex. When no spermatozoa reached the immediate vicinity of the oocyte within 20 min of insemination, another aliquot of capacitated spermatozoa was added.

Preparation of cumulus–oocyte complexes (COCs).

When first retrieved from the ovary, oocyte–cumulus complexes are separate. However, in the oviduct, they adhere to form a single large cumulus mass. Because this mass was too

large to detect fertilizing spermatozoa within it, we separated the mass into smaller individual cumulus–oocyte complexes using a brief (0.5– 2.0 min) treatment with bovine testicular hyaluronidase (Sigma-Aldrich; 80 units/ml at 37°C) with gentle pipetting. In some cases, a large cumulus mass was left in hyaluronidase-free HTF–BSA medium for 1 h (5% CO₂, at 37 °C), allowing the mass to dissociate spontaneously into several individual cumulus masses. These were washed four times with Hepes-buffered HTF (pH 7.35 ± 0.1) containing 0.3% BSA, followed by a final wash with HTF–BSA.

Assessment of acrosomal exocytosis

Acrosomal exocytosis was quantified after in vitro capacitation as previously described (Hirohashi et al., 2015; Muro et al., 2012). Briefly, mouse sperm from transgenic EGFP mice were capacitated for 90 min followed by 30 min incubation with different concentrations of Progesterone (dissolved in DMSO). The percentage of acrosomal exocytosis was determined by flow cytometry. The viable sperm were selected by staining with propidium iodide (final concentration, 10 µg/ml), and their acrosomal integrity was determined by the presence of acrosomal EGFP.

Acrosomal exocytosis in sperm passing through cumulus-oocyte complexes was performed as previously described (Jin et al., 2011). Briefly, oocytes were immobilized on a glass bottom-culture dish under a coverslip supported by silicon grease. The depth of the preparation was adjusted to 100 µm using a stereo microscope. The culture dish was placed in an incubator chamber at 37°C and 5% CO₂, 5% O₂, 90% N₂ (Peltier-4&CO₂, Taiei Electric). The concentration of sperm in the each drop was adjusted to 1-5 x 10⁴/ml.

To image sperm passing through the cumulus, a combination of transmitted light and epifluorescence was used. Mechanical shutters (VS25, Uniblitz), controlled by a pulse generator (VMM-D3J, Uniblitz), were placed at the mercury lamp for epifluorescence optics and at the halogen lamp for transmitted light. The time required for transition

between an open and closed state was ~3 msec. EGFP and Ds-Red2 fluorescence were excited at (460-500) nm and the images collected by a sensitive video camera (NC-R550b, NEC) mounted with a triple electron multiplying charge-coupled device (3EM-CCD) was used to record the movement of sperm.

Sperm within the cumulus cell matrix were viewed on a large screen using transmitted light and were manually kept in focus. After ~90 min of recording (DIGA DMR-XW31, Panasonic), the presence (acrosome intact) or absence (acrosome reacted) of EGFP in each sperm was evaluated by retrospective slow motion analysis of digital movies.

Derivation of average residence time of sperm within COCs

Analysis of digital videos of sperm moving within the cumulus matrix of each COC enabled us to calculate, on average, how long individual sperm remained in the matrix. Given that sperm-sperm interactions were negligible and there was no limit for sperm entry, then the average time spent by sperm within the COCs can be adequately described by a single first-order reaction, as described below.

$$V_t^{\text{out}} = k \times S_t \quad (1)$$

where k and S_t are a correlation coefficient and cell number remaining in COCs at time t , respectively. Also, the rate of change in S_t is given by

$$dS/dt = V_t^{\text{in}} - V_t^{\text{out}} \quad (2)$$

where V_t^{in} designates the velocity of entering sperm into COCs.

$$dS/dt = V_t^{\text{in}} - kS_t \quad (3)$$

$$k^{-1} = S_t / (V_t^{\text{in}} - dS/dt) \quad (4)$$

Derivation of the average residence time

Set $V_t^{\text{in}} = 0$, by removing all sperm outside any time, and watch sperm going out of COCs to evaluate the residence time of individual sperm. Sperm of the residence time τ will escape out of COCs at $t = \tau$. The number of sperm escaping out of COCs at $t = \tau$ within a time window of dt is given by

$$dS = -kS_t dt \quad (5)$$

The average residence time T for all sperm inside at $t = 0$, i.e. S_0 , is therefore given by

$$T = \left(\int_{t=0}^{t=\infty} \tau \, dS \right) / S_0. \quad (6)$$

Using the solution of equation 4, i.e. $S = S_0 \exp(-kt)$ (7)

and replacing dS by $-kSdt$ following equation 5, equation 6 will give

$$T = k^{-1}. \quad (8)$$

The average residence time for total number of sperm (T_{total}) in the defined period (0 – 90 min) is given by

$$T_{\text{total}} = \Sigma (S_t \times k^{-1}) / \Sigma S_t \quad (9)$$

Statistical analysis

Data for each set of experiments are presented as the mean \pm standard error of the mean (SEM) of at least 3 independent replicates. Statistical analyses were performed by One-way ANOVA using the GraphPad Prism Software (San Diego, CA, USA). The level of statistical significance was determined at $p < 0.05$.

Results

Acrosomal exocytosis rarely occurred while sperm were passing through the cumulus in vitro

Because a previous report suggested that most fertilizing sperm do not undergo AE after binding to the ZP, progesterone has remained another favorable candidate for inducing AE. As previously observed, progesterone stimulates the rate of AE in a dose-dependent manner in vitro (Fig.1). The maximum response was achieved using 40 μM of progesterone. In addition, because fertilization rate is higher with cumulus-intact oocytes than with cumulus-denuded oocytes (Jin et al., 2011) and progesterone is a major secretory product from the cumulus cells surrounding the ovulated oocytes, we evaluated if sperm transiting through the cumulus cells would favor the triggering of AE. Thus, we

performed live imaging of transgenic EGFP sperm during in vitro fertilization (IVF) with COCs to determine the occurrence of AE during this transit. Capacitated sperm from transgenic males were used to inseminate COCs and the sperm were monitored continuously using a live imaging system, consisting in an epifluorescence microscope with a supersensitive video camera. It was revealed that both acrosome-intact and acrosome-reacted sperm were capable of entering the cumulus. The accumulative total number of sperm that entered the cumulus matrix over the time and the number remaining in the cumulus matrix at given time points were counted (Fig. 1A). Interestingly, the total number of sperm inside the cumulus at any given time point remained fairly constant (black circles) while the accumulative number of sperm entering the COCs increased over the time, indicating that a large number of sperm was able to leave the cumulus. Approximately 90% of sperm entering the cumulus swam out of it by 100-min post-insemination. The rate of sperm entry into the cumulus decreased with time for acrosome-intact, but kept constant for acrosome-reacted sperm (Fig. 1B). Accordingly, a transition from acrosome-intact to acrosome-reacted in the sperm population in the cumulus matrix occurred within ~60 min post-insemination (Fig. 1C-E). The average residence time in the cumulus, estimated by equations (see Materials and Methods), was 7.1 ± 2.2 min for acrosome-intact sperm and 26.4 ± 4.8 min for the acrosome-reacted sperm (Fig. 1D, Table 1).

Next, we quantify the percentage of sperm undergoing AE while travelling through the cumulus. A total number of 166 sperm reached the ZP periphery with intact acrosome. Similarly, 67 sperm reached that are without the acrosomes (Table 1). However, only 8 out of 166 acrosome intact sperm underwent AE inside the cumulus (4.8%). The rate of AE by sperm in the cumulus was only 7%/h during 90 min following insemination. Because the rate of spontaneous AE in HTF-medium was ~10%/h, it is unlikely that induction of AE was promoted by direct interaction with COC under our IVF condition. Similarly, given that the

in vitro fertilization conditions do not completely reflect what occurs in vivo, the question of site of sperm AE should be addressed within the female reproductive tracts. This led us to examine where AE take place in the oviduct, before sperm reach the COCs.

Time course of in vivo fertilization

To understand where AE occurs in sperm migrating through the oviduct, the numbers and the acrosomal state of sperm were determined in different regions of the oviduct: the utero-tubal junction (UTJ), the lower, middle and upper parts of isthmus, and the ampulla (Figure 3A). The ampulla included the ampullary-isthmic junction. Most of the sperm storage reservoir is located in the lower isthmus. Female reproductive tracts were dissected out after copulation of C57BL/6JxBalBc females with CAG/su9-DsRed2, Acr3-EGFP double knockin males. After mating, a large number of sperm are deposited in the uterus (Fig.3B) and only a limited population of cells can enter the oviduct by crossing the UTJ. Sperm were seen within the lumen of the oviduct 30 - 45 min post coitus and colonized most of the lower segments of the oviduct after 1.5 h post coitus (Figure 3C-D). Because of the transparency of the mouse female reproductive tract and the bright green and red fluorescence of the transgenic sperm, it was possible to record precisely the migration of sperm in excised oviducts using live video imaging (Yamaguchi et al., 2009) (Figure 3C-D). In the first set of experiments, we investigated the “fertilization window” after completion of mating. Ovulated unfertilized and fertilized oocytes were retrieved by flushing the ampulla with culture medium at specific time points after the end of the mating period. The recovered oocytes were incubated for 24 h in 5% CO₂ at 37°C and fertilization was evaluated by assessing the percentage of eggs that reached the two cell stage. We found that after 1.5 h post mating, 0 – 5% of the MII eggs were fertilized. In contrast, after 4 h post mating, around ~40% of oocytes recovered were fertilized. After 7 h post mating,

more than 90% of the oocytes had reached the two-cell stage (Figure 3E), suggesting that fertilization continues for several hours in vivo.

In the next set of experiments, the oviducts were dissected out 1.5 h and 4 h after the mating period and sperm within the oviducts were immediately examined using confocal microscopy to quantify the number of sperm in each segment. As expected from the fertilization window experiments, sperm migration through the oviduct was gradual; i.e., most of the sperm were found in the lower segments of the oviduct (UTJ to middle isthmus) 1.5 h after mating, and then only small numbers of sperm reached at the upper isthmus and ampulla 4 h after mating (Fig 3F-G). When oviducts from naturally ovulated and superovulated females were compared, we found no significant differences in the time-course of sperm migration (Supplementary Figures 1 and 2).

Most of sperm that migrated through the UTJ and formed the sperm reservoir in the isthmus were acrosome intact.

In the UTJ, we observed that sperm migrated through the pockets created by the longitudinal folds (Figure 4 A-C). The heads appeared to adhere to the epithelium but this was not as evident as in other parts of the isthmus (Fig. 4D-E). This was more evident not on the tip of the colliculus tubarius but on the upper parts of the UTJ. Sperm migration into the UTJ seemed to occur within a short period of time (1.5 h) after coitus, because the number of sperm in this region did not increase during next 2.5 h (Fig 3 F-G). Over 97% of the sperm in this region were acrosome-intact, suggesting that acrosomal integrity may be a prerequisite for crossing the UTJ.

After crossing the UTJ, sperm moved to the lower isthmus (Figure 4F-G). This region contained the majority of the sperm and is considered to serve as a sperm reservoir (Suarez, 2002). Sperm were distributed in folds as well as in the central portion of the lumen (Supplementary video 1), in particular, in the region of the lower isthmus proximal to

the UTJ (Figure 4I-K). Sperm in the central portion of the lumen were swimming freely, whereas sperm located in the pockets formed by mucosal folds that were bound to the epithelium (Figure 4 H-J).

It was also observed that a population of sperm were not attached to the oviductal epithelium (Supplementary video 2) while others were firmly attached by the anterior part of the head, where the convex surface of the acrosome arc is located (Supplementary video 3). In other areas of the lower isthmus, we could only observe sperm attached to the epithelium mainly in the mucosal folds (Supplementary video 4).

Similarly to what occur in the UTJ, in the lower isthmus, over 95% of the sperm were acrosome intact.

The region that is located between the sperm reservoir in the lower isthmus and the upper isthmus was arbitrarily called the middle isthmus. In this region, fewer sperm were observed and they were all located the pockets formed by mucosal folds (Figure 4L-O and Supplementary video 5). All of the sperm in this region were attached to the epithelium and as observed in the UTJ and lower isthmus, over 95% of the sperm did not undergo AE.

The analysis of the upper segments of the oviduct revealed that a significant number of sperm underwent AE in the upper isthmus

Very few sperm were detected in the upper isthmus at all time points. Most sperm were attached to the epithelium, although occasionally we observed some freely swimming sperm. Interestingly, in this region, about 35% of sperm did not show green fluorescence, indicating that they had already undergone acrosomal exocytosis (Figure 5).

In the ampulla, very few sperm were detected. At 1.5 h after the mating period, we did not observe any sperm but this does not necessarily mean that the sperm were not arriving to the site of fertilization because at that time, around 3% of the eggs were fertilized. At 4 h,

some sperm were detected in each ampulla in a ratio of 1:1 with the ovulated eggs. Only 5% of the sperm in the ampulla were acrosome intact (Figure 6; Supplementary videos 6 and 7). Occasionally, the red fluorescence of the sperm mitochondria was observed inside the eggs cytoplasm indicating that fertilization occurred (Fig.6 C-E). Other times, we observed more than one sperm surrounding one egg (Fig.6 F-K). A representative image showing the acrosomal status of sperm in the ampulla and in the upper isthmus where both gametes lost their acrosomes is shown in Figure 7. The percentage of acrosome intact sperm at different time points in the different regions of the oviduct is shown in Figure 8.

Discussion

Acrosomal exocytosis is essential for fertilization because it is critical for the appropriate localization of sperm-egg fusion proteins. It has been long thought that AE took place upon interaction with certain proteins from the zona pellucida of the egg, in particular, the protein ZP3 (Arnoult et al., 1996). This idea was supported by many studies where acrosome-intact sperm were reported to bind to the ZP in vitro and then undergo AE (Florman and Storey, 1982; Saling et al., 1979; Storey et al., 1984), but most importantly, by the fact that solubilized ZP binds specifically to the acrosomal region of sperm head and triggers AE (Bleil and Wassarman, 1983; Mortillo and Wassarman, 1991). Thus, many studies for understanding the process of AE were performed in vitro using a non-physiological form of the proposed stimulant of the process.

Baibakov and colleagues challenged the concept of ZP-induced AE by demonstrating that binding of mouse sperm to intact ZP is not sufficient to induce AE (Baibakov et al., 2007). The authors proposed a mechanosensory mechanism by which passage through the ZP matrix would induce AE and produce the loss of the acrosomal shroud. This observation,

where acrosome intact sperm bind to the ZP and remain substantially intact, was also reported many years ago by another group (Storey et al., 1984). These results however were only limited to the observation of the sperm bound to the ZP in the absence of cumulus. Using [BDF1-Tg (CAG-mtDsRed2, Acr-EGFP) RBGS0020sb male mice that produced sperm with green fluorescent labeling of acrosomes and red fluorescent labeling of flagellar midpiece mitochondria, Jin and colleagues (Jin et al., 2011) made a groundbreaking observation claiming that most fertilizing sperm initiated AE before interacting with the ZP. In this study, however, it was not reported if AE in fertilizing spermatozoa occurred within the extracellular matrix of the cumulus although many reports were stating that possibility as a fact (Chen et al., 2013; Gadella, 2012). Similar results were also obtained many years ago using rabbit sperm (Kuzan et al., 1984). Using guinea pig and mouse sperm, it was also demonstrated that sperm that underwent AE bind and penetrate the ZP (Huang et al., 1981; Inoue et al., 2011).

These evidence open four possible scenarios where sperm may undergo acrosomal exocytosis while travelling to the site of fertilization: a **First scenario**, where sperm undergo exocytosis at the ZP surface by ZP3; A **second scenario** where sperm undergo AE within the cumulus by cellular or acellular factors or at the surface of cumulus by cumulus matrix and soluble factors; a **third scenario**, where sperm undergo AE in the vicinity of cumulus by soluble factors from cumulus and/or oviductal milieu (Buffone et al., 2014). Currently, there is strong evidence suggesting that the first scenario would not be the prevalent in mouse sperm, although this hypothesis remained to be confirmed by in vivo studies. Considering the second scenario, we aimed to investigate the occurrence of AE while capacitated sperm were swimming through the cumulus cells. Progesterone is actively produced by cumulus cells after ovulation and its concentration within the cumulus matrix is in the order of micro molar range (Kobori et al., 2000; Miska et al., 1994). Using a live imaging system, we observed that very few sperm underwent AE within cumulus cells

despite of the high concentration of progesterone present in that location. The rate of AE was not different to what is normally observed as spontaneous AE in the incubation medium. Previous reports showed that the sperm protein NYD-SP8-induced a Ca^{2+} mobilization in the cumulus cells that would result in progesterone release, which in turn induces the AE (Sun et al., 2011). Others also reported that fibronectin present in the cumulus matrix would also induce AE (Diaz et al., 2007). Without precluding these possibilities, our results demonstrated that most of the sperm do not undergo AE upon interaction with the cumulus cells or with certain components of the matrix. This conclusion would suggest that the second scenario is not the prevalent model where most of the sperm undergo AE. However, it is mandatory to evaluate this process in vivo because of several fundamental reasons: i) although our live imaging system using cumulus enclosed eggs is extremely useful, this situation does not take into consideration that the physiological site for this process is the oviduct; ii) the sperm-egg ratio in the ampulla is reported to be close to 1:1 (Stewart-Savage and Bavister, 1988), and in our system, around a 50 - 100 sperm were inseminated per single oocyte; iii) we inseminated in vitro capacitated sperm, without considering that in vivo, sperm are ejaculated and interact with proteins and molecules present in the seminal plasma and the uterine/oviductal fluids. And more important, ejaculated sperm have to go through the UTJ, where a small group of sperm are selected by unknown mechanisms; iv) capacitation inside the oviduct might be completely different compared to capacitation in vitro: for instance, in vivo, selected sperm are capacitated during a close sperm-oviduct epithelium interaction. For all these reasons, we decided to evaluate this process in vivo using natural mating which will also let us confirm our in vitro results suggesting that most of the sperm do not undergo AE within the cumulus but also, to evaluate the occurrence of the third scenario: sperm undergoing AE prior to encountering the COC.

Of the millions of sperm normally ejaculated in natural mating, only a few hundreds reach the isthmus of the oviduct, where most of them are stored in a reservoir. Only a few reach the ampulla at the time of fertilization. Taking advantage of the powerful capabilities of the double transgenic mice containing EGFP in the acrosome and DsRed2 in the mitochondria, it was possible to follow the sperm and their acrosomal status while transiting to the ampulla. First, as observed by others, very few sperm can reach the lower isthmus after crossing the UTJ. According to our results, only acrosome intact sperm were observed in the UTJ or in the lower isthmus suggesting that at least in part, some of the features that an ejaculated sperm might possess in order to cross the UTJ, is to be acrosome intact. Little is known about mechanisms governing the crossing through the UTJ, but It is well established that there are critical sperm components that are necessary for this passage such as the protein ADAM3 and other proteins that are ultimately related to its expression (Cho et al., 1998; Ikawa et al., 2011; Marcello et al., 2011; Nishimura et al., 2004; Shamsadin et al., 1999; Tokuhiko et al., 2012) .

There is strong evidence from multiple species that the oviductal reservoir is created by binding of sperm to oviductal epithelium (Suarez, 2002). In the lower isthmus, is certainly clear that most of the sperm are firmly attached to the epithelium while others are swimming freely and virtually all the sperm in this region are acrosome intact. Previous reports claimed that those sperm that are not attached to the epithelium, the incidence of AE is high (Esponda and Moreno, 1998). However, using EGFP sperm, we could not observe that difference. It is certainly not clear how, the nature of the sperm binding to the epithelium controls both, the capacitation process as well as, the maintenance of sperm with intact acrosomes. Previous experiments using guinea pig sperm showed that sperm capacitation proceeds at a faster rate when mating occurs after ovulation suggesting that there is a tight mechanism of control of this process (Smith and Yanagimachi, 1989).

Little is known about sperm release from the epithelium for fertilization. What is clearly evident based on our results is that, after leaving the reservoir, where hyperactivated motility may play a significant role (Suarez, 2008), sperm tend to localize in the oviductal fold, as observed in the middle isthmus. Here, fewer sperm were observed and all of them were still acrosome intact. Hyperactivation plays an essential role in the progression of sperm throughout the oviduct since Catsper-null sperm are able to cross the UTJ but they hardly progress upper in the isthmus (Ho et al., 2009). Hyperactivation may provide the force necessary for overcoming the binding between sperm and oviductal epithelium.

Once the very few sperm reached the upper segments of the isthmus, we noted that around 40 % of the sperm were acrosome reacted. Sperm in this region were usually attached to the epithelium but other times, they were freely swimming. This is the first area in the oviduct where we observed a higher proportion of acrosome reacted sperm. Those sperm that left the upper isthmus and move upward to the ampulla were mostly acrosome reacted, suggesting that the physiological AE might take place in the upper segments of the oviduct. Supporting our observations, Yanagimachi and Mahi (Yanagimachi and Mahi, 1976) demonstrated that regardless of the time of insemination, the spermatozoa participating in fertilization appeared to undergo the acrosome reaction after they reached the proximal part of the oviduct or when they were very near the eggs. Along this line, over 95% of the sperm that reached the ampulla already underwent the AE prior to encounter with the cumulus enclosed eggs. These observations support our in vitro studies using cumulus cells and the studies by others, where the fertilizing sperm underwent AE prior to binding to ZP. However, very few sperm were able to reach the ampulla with intact acrosomes, suggesting that it is possible that other physiological mechanism may ensure the induction of acrosomal exocytosis in the ampulla to promote fertilization.

What stimuli/s is/are triggering exocytosis in this region remains an enigma although progesterone might be a candidate since it is produced by cumulus cells and may diffuse downstream toward the sperm. The reason why sperm in the lower segments of the oviduct did not undergo AE may be related to unknown mechanisms related to the sperm binding to the epithelium or, to the progesterone concentration in the environment of these regions of the oviduct. The downstream flow of oviductal fluid described recently may be necessary for initiating the mechanisms of rheotaxis (Miki and Clapham, 2013) but also, to create a progesterone gradient that is essential for sperm chemotaxis (Guidobaldi et al., 2008; Oren-Benaroya et al., 2008; Teves et al., 2006). The reason that the sperm in the oviduct are not reacted by progesterone action is probably due to its concentration. The low concentration of progesterone (pico molar range) that is necessary for chemotaxis is not sufficient for inducing the AE, because we observed that it is needed at least a concentration of 10 μ M of this steroid to induce AE.

In summary, by combining our in vitro and ex vivo results, we demonstrated that: i) using a live imaging system, that the rate of AE of sperm swimming through the cumulus cells is similar to what occurs in a capacitating media without any substance that induce the AE (spontaneous AE); ii) that most of the sperm undergo AE in the upper segment of the oviductal isthmus, prior to entering the cumulus mass.

Acknowledgments:

We would like to thank Dr George Gerton for his insightful comments. We also would like to thank Drs. Shoji Baba, Dr. Pablo Pomata, Dr Gabriel Rabinovich, Dr. Diego Crocci, Dr. Juan P. Cerliani and Trinidad Suarez for their technical assistance.

Figure Legends

Figure 1: Progesterone stimulates the acrosomal exocytosis in a dose dependent manner. Mouse sperm from transgenic EGFP mice were capacitated for 90 min followed by 30 min incubation with different concentrations of Progesterone. The percentage of acrosomal exocytosis was determined by flow cytometry. The viable sperm were selected by staining with propidium iodide (final concentration, 10 $\mu\text{g/ml}$), and their acrosomal integrity was determined by the presence of acrosomal EGFP. Data represent the mean \pm standard error of the mean (SEM; $n = 4$ experiments).

Figure 2: Characterization of sperm migration through the cumulus matrix in vitro according to the acrosomal status. **a)** The plots represent the cumulative number of sperm entering the COCs (open circles) and the number of sperm remaining in the COCs (closed diamonds) at given times after insemination. The COCs area was drawn as a broken circle as shown in e. **b)** In the analysis of type of sperm entering the COCs, an apparent logistic increase of acrosome-intact sperm (green), and a relatively low but constant increase of acrosome-reacted sperm (orange), were seen. **c)** In respect to the sperm number remaining in the COCs, acrosome-intact sperm (green) reached a maximum at ~ 40 min post-insemination, followed by the rapid accumulation of acrosome-reacted sperm (orange). **d)** A representative time course of the average residence time of acrosome-intact (green) and reacted (orange) sperm in CCL estimated from equations (Materials & Methods). **e)** Representative photographs show a transition of the sperm population (from acrosome-intact to acrosome-reacted) as a function of time; scale bar, 100 μm .

Figure 3: Evaluation of the timing of in vivo fertilization in mouse. A) Representative diagram showing the different parts of the oviduct that were evaluated in this study; B) Representative image of a cross section of the uterus. Sperm were deposited in the uterus after natural mating. C and D). Transgenic sperm in the uterus and the oviduct after natural mating. The EGFP (C) and the DsRed2 (D) fluorescence is visible through the uterus and oviductal walls. Most of the sperm are located in the uterus while very few cross the UTJ and locate in the lower isthmus. E) Time course of in vivo fertilization. The ovulated eggs were removed from the ampulla after 1.5, 4 or 7 h post mating and incubated in culture medium for 24 h. Then, the percentage of two-cell embryos was recorded. F) Number of sperm quantified using z-stacks images of confocal microscopy in each segment of the oviduct after 1.5 h post mating. G) Number of sperm quantified using z-stacks images of confocal microscopy in each segment of the oviduct after 4 h post mating. Data represent the mean \pm standard error of the mean (SEM; $n = 5$ experiments).

Figure 4: Sperm migration through the UTJ and Isthmus. A) Bright field image of the uterus, UTJ and lower segment of the isthmus. The arrow indicates the colliculus tubarius (CT) protruding into the uterine lumen. B) DsRed2 fluorescence of the image shown in A. Sperm tend to migrate through the UTJ in the pockets between mucosal folds. The arrow in B indicates the mucosal fold where most of the sperm are located. C) EGFP fluorescence of the image shown in A. Most of the sperm in this region have substantially intact acrosomes. D) Cross section of the UTJ after 1.5 h post mating E). Higher magnification of the area depicted in D. Most of the sperm in this region are acrosome intact. F) Bright field representative image the lower isthmus. G and H) DsRed2 and EGFP Fluorescence images of 3A respectively. I) Bright field image of a frozen section of the lower isthmus. Sperm were distributed in folds as well as in the central portion of the lumen, in particular, in the region of the lower isthmus that is close to the UTJ. Sperm that locate in the lumen

were swimming freely in contrast to the sperm that were located in the folds that were epithelium-bound sperm. In J, higher magnification image of the area depicted in I. In K, it is shown a representative fluorescent image (merge of DAPI, EGFP and DsRed2) of a cross section of the lower isthmus showing the acrosome intact sperm located in the oviductal folds. The right arrow indicates the oviductal fold. The left arrow indicates the oviductal wall. L) Representative confocal image of a cross section of the middle oviductal isthmus after 4 h post mating. M) Higher magnification image of the area depicted in L. N) Representative bright field image of the middle isthmus. O) Confocal images showing transgenic sperm located in the oviductal folds (arrow).

Figure 5: The number of acrosome reacted sperm increases in the upper isthmus. In A (brightfield) and B (Fluorescent) are shown representative images of confocal microscopy showing very few sperm in the upper isthmus. Note that the number of sperm is markedly different compared to what is observed in the middle isthmus (panel A, bottom left corner). Some of them underwent acrosomal exocytosis. In C, a higher magnification of sperm showed in B where around 40% of the sperm underwent acrosomal exocytosis prior to entering the ampulla. AR: acrosome reacted; AI: acrosome intact.

Figure 6: Most of the sperm in the ampulla underwent acrosomal exocytosis. A) Representative image of an ampulla after ovulation. The eggs were easily observed through the oviductal wall (B). In C-E, representative images of a fertilized egg where it was possible to observe the fluorescence of the tail. F-H: representative images of two sperm in the vicinity of an egg. Both sperm lost their acrosomes. I-K: representative images of two sperm in the vicinity of an egg. In this case, one sperm was acrosome intact (AI) while the other already underwent acrosomal exocytosis (AR). L-N. A representative

example of one acrosome reacted sperm swimming through 3 ovulated eggs (indicated by arrows). BF: brightfield image,

Figure 7: Representative image showing the acrosomal status of sperm in the upper segments of the oviduct. A) Bright field image of the ampulla and the upper isthmus 4 hours post mating. The areas depicted in this region are shown in B, C and D. B) Bright field, and fluorescence images (left to right) of a representative example of one acrosome reacted sperm (arrow) in the upper isthmus, prior to entering in the ampulla. C and D) Bright field, and fluorescence images (left to right) of two representative examples of one acrosome reacted sperm (arrow) approaching one ovulated MII egg in the ampulla.

Figure 8: Most of the sperm underwent acrosomal exocytosis in the upper segments of the oviductal isthmus. Percentage of sperm that undergo acrosomal exocytosis in the different section of the oviduct after 1.5 h and 4 h post natural mating. UTJ; utero-tubal junction; LI: lower isthmus; MI: middle isthmus; UP: upper isthmus; AMP: ampulla. Results are expressed as the mean \pm standard deviation of 8 independent experiments.

Supplementary material

Supplementary video 1: An example of sperm inside the lower isthmus of the oviduct.

Supplementary video 2: Two different populations of sperm in the lower isthmus: attached to the epithelium and non-attached (free swimming).

Supplementary video 3: An example of acrosome-intact sperm attached to the epithelium.

Supplementary video 4: Sperm located in the mucosal fold of the lower isthmus.

Supplementary video 5: Sperm located in the lower and middle isthmus.

Supplementary video 6: Three sperm in the ampulla in the vicinity of MII-eggs. All of them lost their acrosomes.

Supplementary video 7: Two sperm in the vicinity of one MII-egg. In this case, one sperm is acrosome intact and the other already underwent acrosomal exocytosis.

References

Arnoult, C., Zeng, Y., and Florman, H.M. (1996). ZP3-dependent activation of sperm cation channels regulates acrosomal secretion during mammalian fertilization. *J. Cell Biol.* *134*, 637–645.

Austin, C.R. (1951). Observations on the penetration of the sperm in the mammalian egg. *Aust. J. Sci. Res. Ser B Biol. Sci.* *4*, 581–596.

Baibakov, B., Gauthier, L., Talbot, P., Rankin, T.L., and Dean, J. (2007). Sperm binding to the zona pellucida is not sufficient to induce acrosome exocytosis. *Dev. Camb. Engl.* *134*, 933–943.

Bleil, J.D., and Wassarman, P.M. (1983). Sperm-egg interactions in the mouse: sequence of events and induction of the acrosome reaction by a zona pellucida glycoprotein. *Dev. Biol.* *95*, 317–324.

Buffone, M.G., Foster, J.A., and Gerton, G.L. (2008). The role of the acrosomal matrix in fertilization. *Int. J. Dev. Biol.* *52*, 511–522.

Buffone, M.G., Ijiri, T.W., Cao, W., Merdiushev, T., Aghajanian, H.K., and Gerton, G.L. (2012). Heads or tails? Structural events and molecular mechanisms that promote mammalian sperm acrosomal exocytosis and motility. *Mol. Reprod. Dev.* *79*, 4–18.

Buffone, M.G., Hirohashi, N., and Gerton, G.L. (2014). Unresolved questions concerning mammalian sperm acrosomal exocytosis. *Biol. Reprod.* *90*, 112.

Chang, M.C. (1951). Fertilizing capacity of spermatozoa deposited into the fallopian tubes. *Nature* *168*, 697–698.

Chen, H., Kui, C., and Chan, H.C. (2013). Ca²⁺ mobilization in cumulus cells: role in oocyte maturation and acrosome reaction. *Cell Calcium* *53*, 68–75.

Cherr, G.N., Lambert, H., Meizel, S., and Katz, D.F. (1986). In vitro studies of the golden hamster sperm acrosome reaction: completion on the zona pellucida and induction by homologous soluble zonae pellucidae. *Dev. Biol.* 114, 119–131.

Cho, C., Bunch, D.O., Faure, J.E., Goulding, E.H., Eddy, E.M., Primakoff, P., and Myles, D.G. (1998). Fertilization defects in sperm from mice lacking fertilin beta. *Science* 281, 1857–1859.

Dam, A.H.D.M., Feenstra, I., Westphal, J.R., Ramos, L., van Golde, R.J.T., and Kremer, J. a. M. (2007). Globozoospermia revisited. *Hum. Reprod. Update* 13, 63–75.

Diaz, E.S., Kong, M., and Morales, P. (2007). Effect of fibronectin on proteasome activity, acrosome reaction, tyrosine phosphorylation and intracellular calcium concentrations of human sperm. *Hum. Reprod. Oxf. Engl.* 22, 1420–1430.

Esponda, P., and Moreno, M. (1998). Acrosomal status of mouse spermatozoa in the oviductal isthmus. *J. Exp. Zool.* 282, 360–366.

Florman, H.M., and Storey, B.T. (1982). Mouse gamete interactions: the zona pellucida is the site of the acrosome reaction leading to fertilization in vitro. *Dev. Biol.* 91, 121–130.

Gadella, B.M. (2012). Dynamic regulation of sperm interactions with the zona pellucida prior to and after fertilisation. *Reprod. Fertil. Dev.* 25, 26–37.

Guidobaldi, H.A., Teves, M.E., Uñates, D.R., Anastasia, A., and Giojalas, L.C. (2008). Progesterone from the cumulus cells is the sperm chemoattractant secreted by the rabbit oocyte cumulus complex. *PLoS One* 3, e3040.

Hasuwa, H., Muro, Y., Ikawa, M., Kato, N., Tsujimoto, Y., and Okabe, M. (2010). Transgenic mouse sperm that have green acrosome and red mitochondria allow visualization of sperm and their acrosome reaction in vivo. *Exp. Anim. Jpn. Assoc. Lab. Anim. Sci.* 59, 105–107.

Hirohashi, N., Spina, F.A.L., Romarowski, A., and Buffone, M.G. (2015). Redistribution of the intra-acrosomal EGFP before acrosomal exocytosis in mouse spermatozoa. *Reprod. Camb. Engl.* 149, 657–663.

Ho, K., Wolff, C.A., and Suarez, S.S. (2009). CatSper-null mutant spermatozoa are unable to ascend beyond the oviductal reservoir. *Reprod. Fertil. Dev.* 21, 345–350.

Huang, T.T., Fleming, A.D., and Yanagimachi, R. (1981). Only acrosome-reacted spermatozoa can bind to and penetrate zona pellucida: a study using the guinea pig. *J. Exp. Zool.* 217, 287–290.

Ikawa, M., Tokuhira, K., Yamaguchi, R., Benham, A.M., Tamura, T., Wada, I., Satouh, Y., Inoue, N., and Okabe, M. (2011). Calsperin is a testis-specific chaperone required for sperm fertility. *J. Biol. Chem.* 286, 5639–5646.

Inoue, N., Satouh, Y., Ikawa, M., Okabe, M., and Yanagimachi, R. (2011). Acrosome-reacted mouse spermatozoa recovered from the perivitelline space can fertilize other eggs. *Proc. Natl. Acad. Sci. U. S. A.* 108, 20008–20011.

Jin, M., Fujiwara, E., Kakiuchi, Y., Okabe, M., Satouh, Y., Baba, S.A., Chiba, K., and Hirohashi, N. (2011). Most fertilizing mouse spermatozoa begin their acrosome reaction before contact with the zona pellucida during in vitro fertilization. *Proc. Natl. Acad. Sci. U. S. A.* 108, 4892–4896.

Kang-Decker, N., Mantchev, G.T., Juneja, S.C., McNiven, M.A., and van Deursen, J.M. (2001). Lack of acrosome formation in Hrb-deficient mice. *Science* 294, 1531–1533.

Kobori, H., Miyazaki, S., and Kuwabara, Y. (2000). Characterization of intracellular Ca(2+) increase in response to progesterone and cyclic nucleotides in mouse spermatozoa. *Biol. Reprod.* 63, 113–120.

Kuzan, F.B., Fleming, A.D., and Seidel, G.E., Jr (1984). Successful fertilization in vitro of fresh intact oocytes by perivitelline (acrosome-reacted) spermatozoa of the rabbit. *Fertil. Steril.* 41, 766–770.

Lin, Y.-N., Roy, A., Yan, W., Burns, K.H., and Matzuk, M.M. (2007). Loss of zona pellucida binding proteins in the acrosomal matrix disrupts acrosome biogenesis and sperm morphogenesis. *Mol. Cell. Biol.* 27, 6794–6805.

Marcello, M.R., Jia, W., Leary, J.A., Moore, K.L., and Evans, J.P. (2011). Lack of tyrosylprotein sulfotransferase-2 activity results in altered sperm-egg interactions and loss of ADAM3 and ADAM6 in epididymal sperm. *J. Biol. Chem.* 286, 13060–13070.

Mayorga, L.S., Tomes, C.N., and Belmonte, S.A. (2007). Acrosomal exocytosis, a special type of regulated secretion. *IUBMB Life* 59, 286–292.

Miki, K., and Clapham, D.E. (2013). Rheotaxis guides mammalian sperm. *Curr. Biol. CB* 23, 443–452.

Miska, W., Fehl, P., and Henkel, R. (1994). Biochemical and immunological characterization of the acrosome reaction-inducing substance (ARIS) of hFF. *Biochem. Biophys. Res. Commun.* 199, 125–129.

Mortillo, S., and Wassarman, P.M. (1991). Differential binding of gold-labeled zona pellucida glycoproteins mZP2 and mZP3 to mouse sperm membrane compartments. *Dev. Camb. Engl.* 113, 141–149.

Muro, Y., Buffone, M.G., Okabe, M., and Gerton, G.L. (2012). Function of the acrosomal matrix: zona pellucida 3 receptor (ZP3R/sp56) is not essential for mouse fertilization. *Biol. Reprod.* 86, 1–6.

Nishimura, H., Kim, E., Nakanishi, T., and Baba, T. (2004). Possible function of the ADAM1a/ADAM2 Fertilin complex in the appearance of ADAM3 on the sperm surface. *J. Biol. Chem.* *279*, 34957–34962.

Oren-Benaroya, R., Orvieto, R., Gakamsky, A., Pinchasov, M., and Eisenbach, M. (2008). The sperm chemoattractant secreted from human cumulus cells is progesterone. *Hum. Reprod. Oxf. Engl.* *23*, 2339–2345.

Osman, R.A., Andria, M.L., Jones, A.D., and Meizel, S. (1989). Steroid induced exocytosis: the human sperm acrosome reaction. *Biochem. Biophys. Res. Commun.* *160*, 828–833.

Ren, D., Navarro, B., Perez, G., Jackson, A.C., Hsu, S., Shi, Q., Tilly, J.L., and Clapham, D.E. (2001). A sperm ion channel required for sperm motility and male fertility. *Nature* *413*, 603–609.

Roldan, E.R., Murase, T., and Shi, Q.X. (1994). Exocytosis in spermatozoa in response to progesterone and zona pellucida. *Science* *266*, 1578–1581.

Saling, P.M., Sowinski, J., and Storey, B.T. (1979). An ultrastructural study of epididymal mouse spermatozoa binding to zonae pellucidae in vitro: sequential relationship to the acrosome reaction. *J. Exp. Zool.* *209*, 229–238.

Satouh, Y., Inoue, N., Ikawa, M., and Okabe, M. (2012). Visualization of the moment of mouse sperm-egg fusion and dynamic localization of IZUMO1. *J. Cell Sci.* *125*, 4985–4990.

Shamsadin, R., Adham, I.M., Nayernia, K., Heinlein, U.A., Oberwinkler, H., and Engel, W. (1999). Male mice deficient for germ-cell cyritestin are infertile. *Biol. Reprod.* *61*, 1445–1451.

Smith, T.T., and Yanagimachi, R. (1989). Capacitation status of hamster spermatozoa in the oviduct at various times after mating. *J. Reprod. Fertil.* *86*, 255–261.

Sosnik, J., Miranda, P.V., Spiridonov, N.A., Yoon, S.-Y., Fissore, R.A., Johnson, G.R., and Visconti, P.E. (2009). Tssk6 is required for Izumo relocalization and gamete fusion in the mouse. *J. Cell Sci.* *122*, 2741–2749.

Stewart-Savage, J., and Bavister, B.D. (1988). Success of fertilization in golden hamsters is a function of the relative gamete ratio. *Gamete Res.* *21*, 1–10.

Storey, B.T., Lee, M.A., Muller, C., Ward, C.R., and Wirtshafter, D.G. (1984). Binding of mouse spermatozoa to the zonae pellucidae of mouse eggs in cumulus: evidence that the acrosomes remain substantially intact. *Biol. Reprod.* *31*, 1119–1128.

Suarez, S.S. (2002). Formation of a reservoir of sperm in the oviduct. *Reprod. Domest. Anim. Zuchthyg.* *37*, 140–143.

Suarez, S.S. (2008). Control of hyperactivation in sperm. *Hum. Reprod. Update* 14, 647–657.

Sun, T.T., Chung, C.M., and Chan, H.C. (2011). Acrosome reaction in the cumulus oophorus revisited: involvement of a novel sperm-released factor NYD-SP8. *Protein Cell* 2, 92–98.

Teves, M.E., Barbano, F., Guidobaldi, H.A., Sanchez, R., Miska, W., and Giojalas, L.C. (2006). Progesterone at the picomolar range is a chemoattractant for mammalian spermatozoa. *Fertil. Steril.* 86, 745–749.

Tokuhiro, K., Ikawa, M., Benham, A.M., and Okabe, M. (2012). Protein disulfide isomerase homolog PDILT is required for quality control of sperm membrane protein ADAM3 and male fertility [corrected]. *Proc. Natl. Acad. Sci. U. S. A.* 109, 3850–3855.

Yamaguchi, R., Muro, Y., Isotani, A., Tokuhiro, K., Takumi, K., Adham, I., Ikawa, M., and Okabe, M. (2009). Disruption of ADAM3 impairs the migration of sperm into oviduct in mouse. *Biol. Reprod.* 81, 142–146.

Yanagimachi, R. (2011). Mammalian sperm acrosome reaction: where does it begin before fertilization? *Biol. Reprod.* 85, 4–5.

Yanagimachi, R., and Mahi, C.A. (1976). The sperm acrosome reaction and fertilization in the guinea-pig: a study in vivo. *J. Reprod. Fertil.* 46, 49–54.

Figure 1

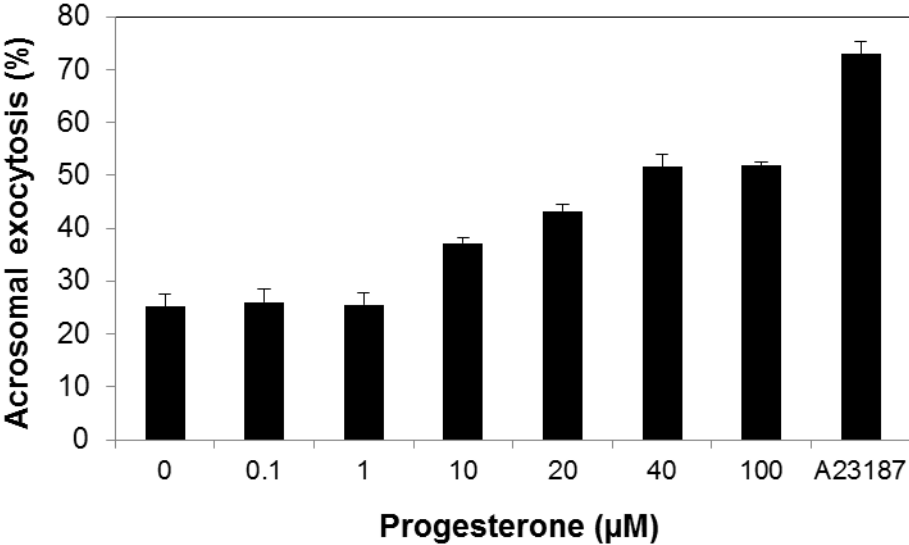
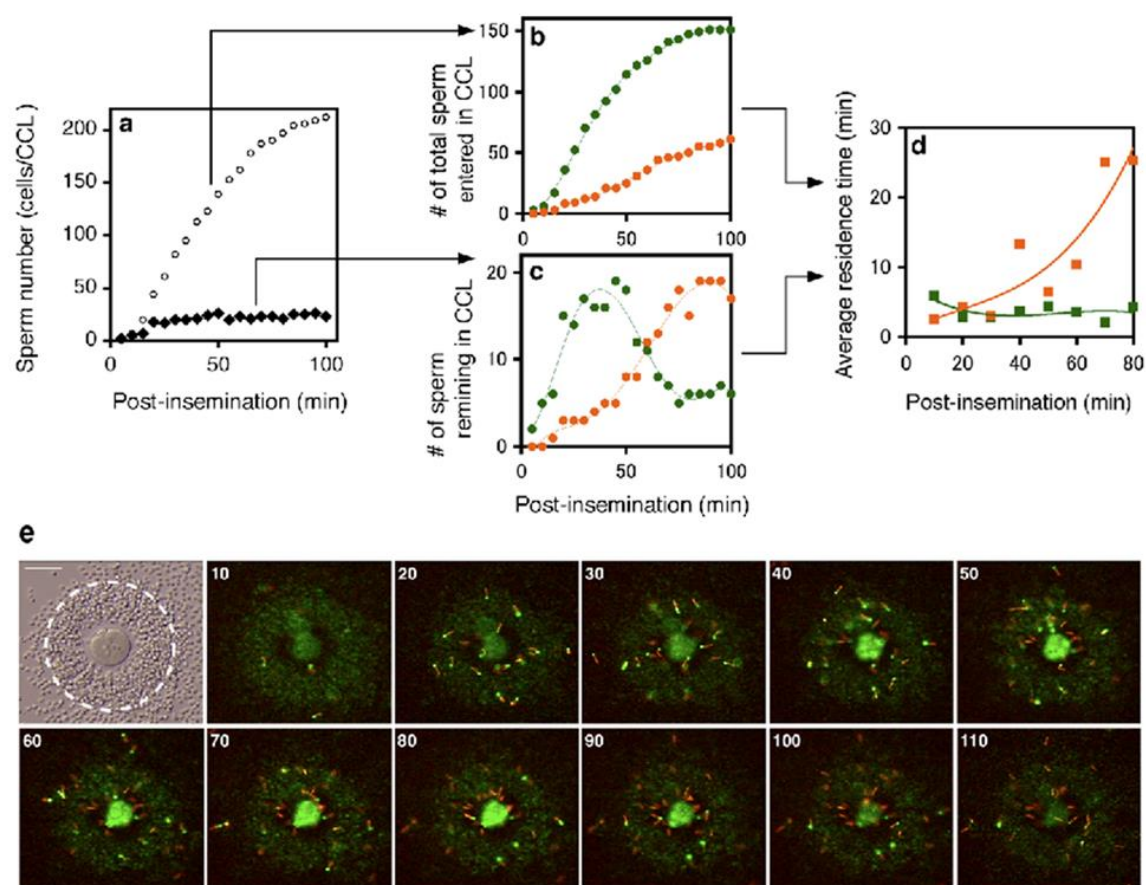


Figure 2



Average residence time in the COCs for AI sperm (min)	7.1 ± 2.2
Average residence time in the COCs for AR sperm (min)	26.4 ± 4.8
Number of sperm that entered the COCs	233 (100 %)
Number of sperm that entered the COCs with Acrosome	166 (71.3 %)
Number of sperm that entered the COCs without the acrosome	67 (28.7 %)
Total number of sperm that trigger AE in the COCs	8 (4.8 %)
Rate of AE in HTF medium (%/ hour)	10
Rate of AE in cumulus matrix (%/ hour)	7

Table 1: Acrosomal exocytosis of sperm travelling through the cumulus cells matrix. Data represent 26 experiments (n=26). Average residence time is expressed as the mean ± SEM. AI: acrosome intact sperm; AR: acrosome reacted sperm.

Figure 3

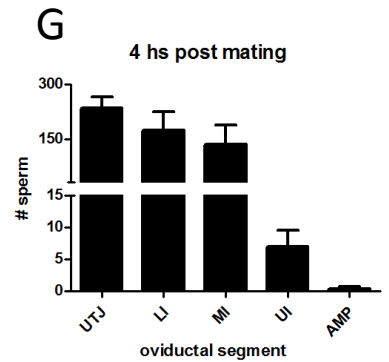
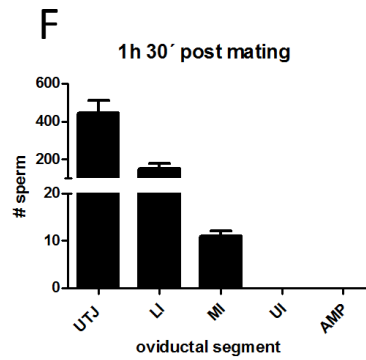
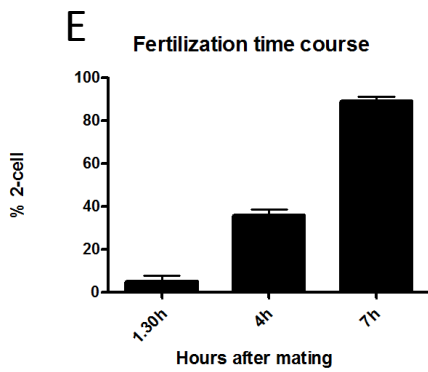
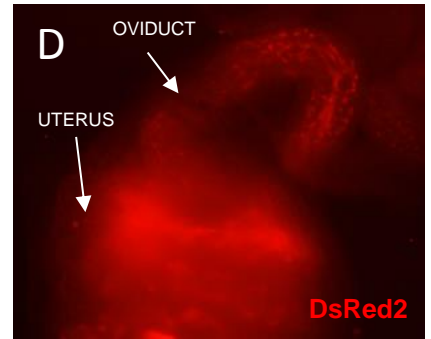
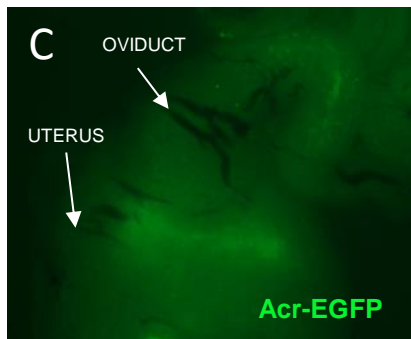
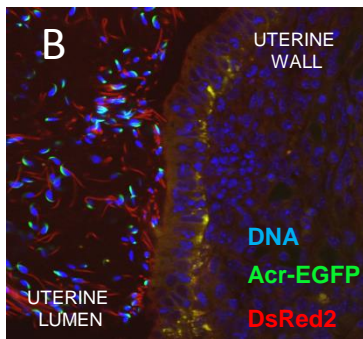
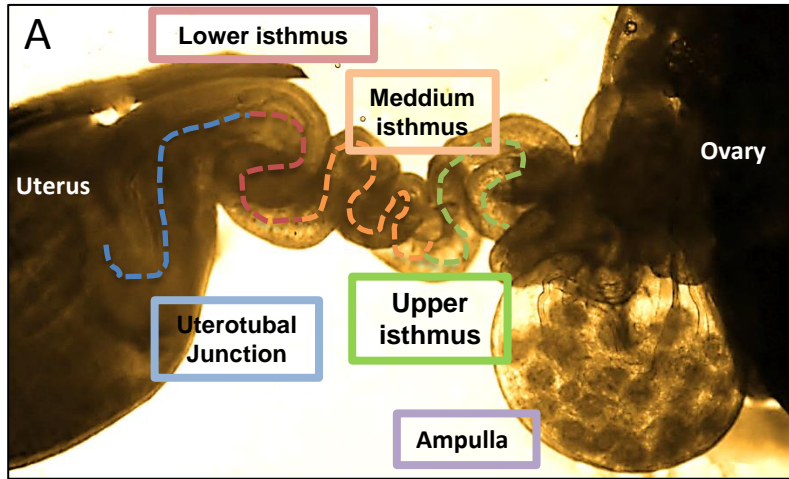


Figure 4

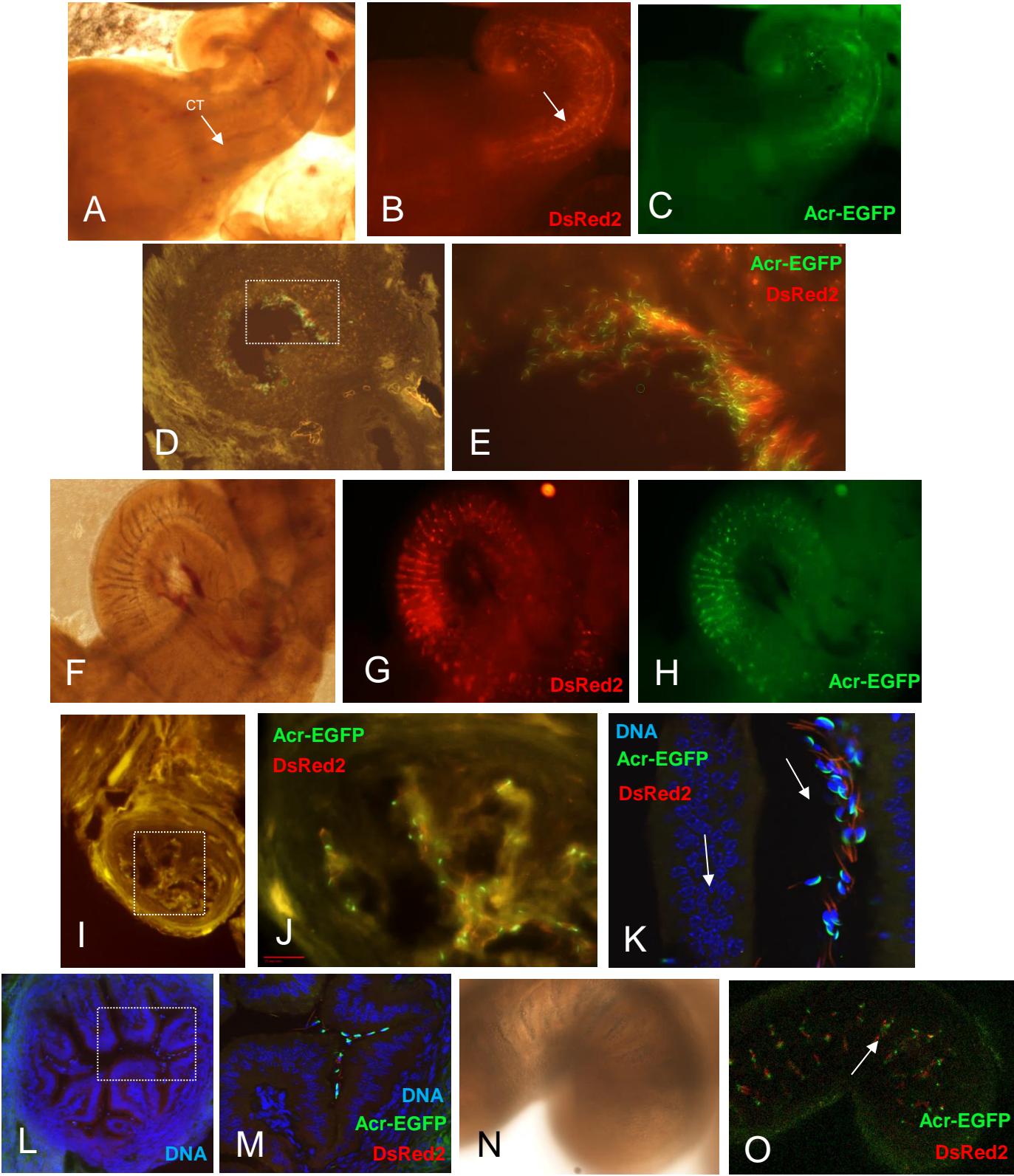


Figure 5

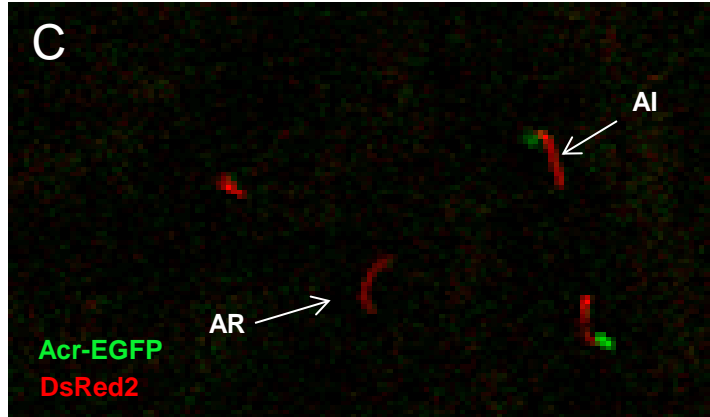
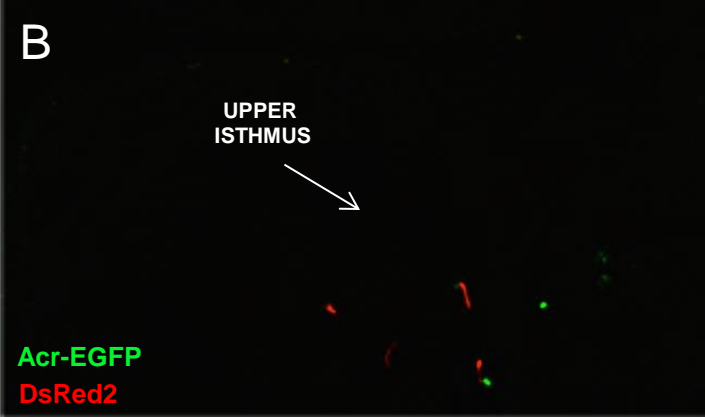
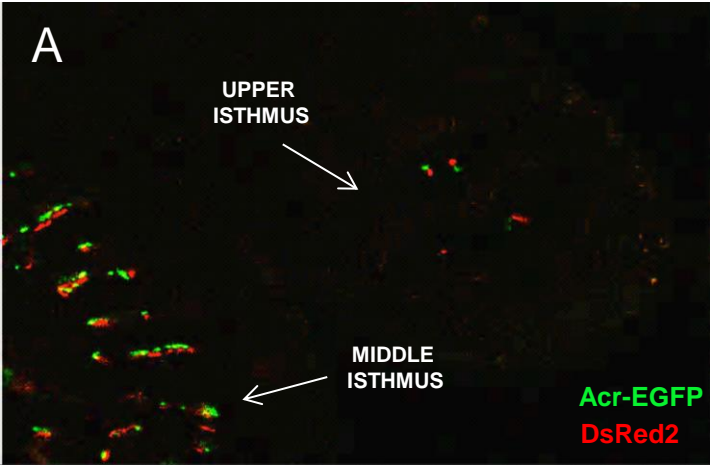
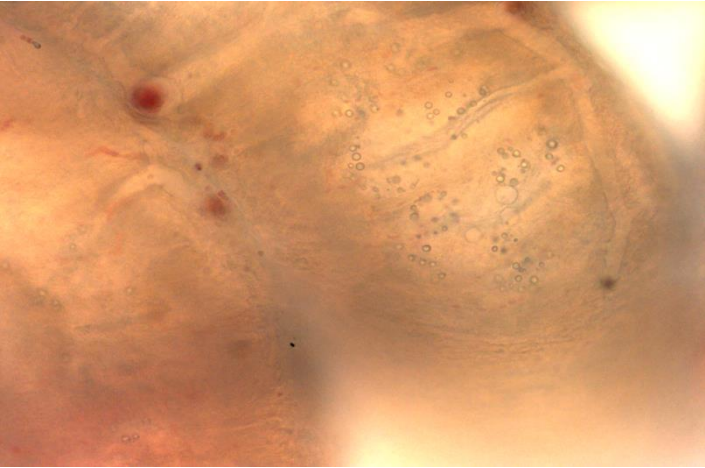


Figure 6

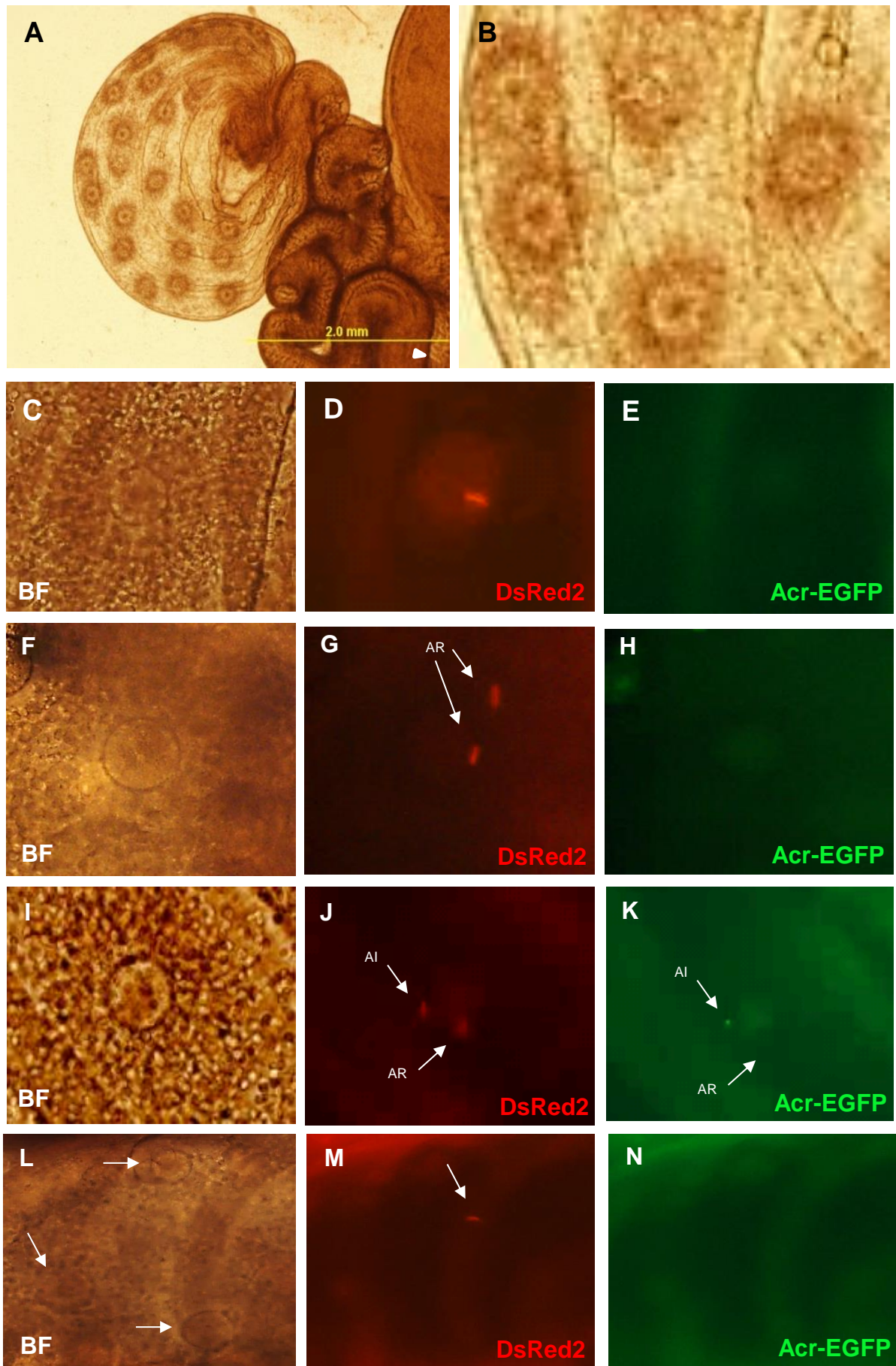


Figure 7

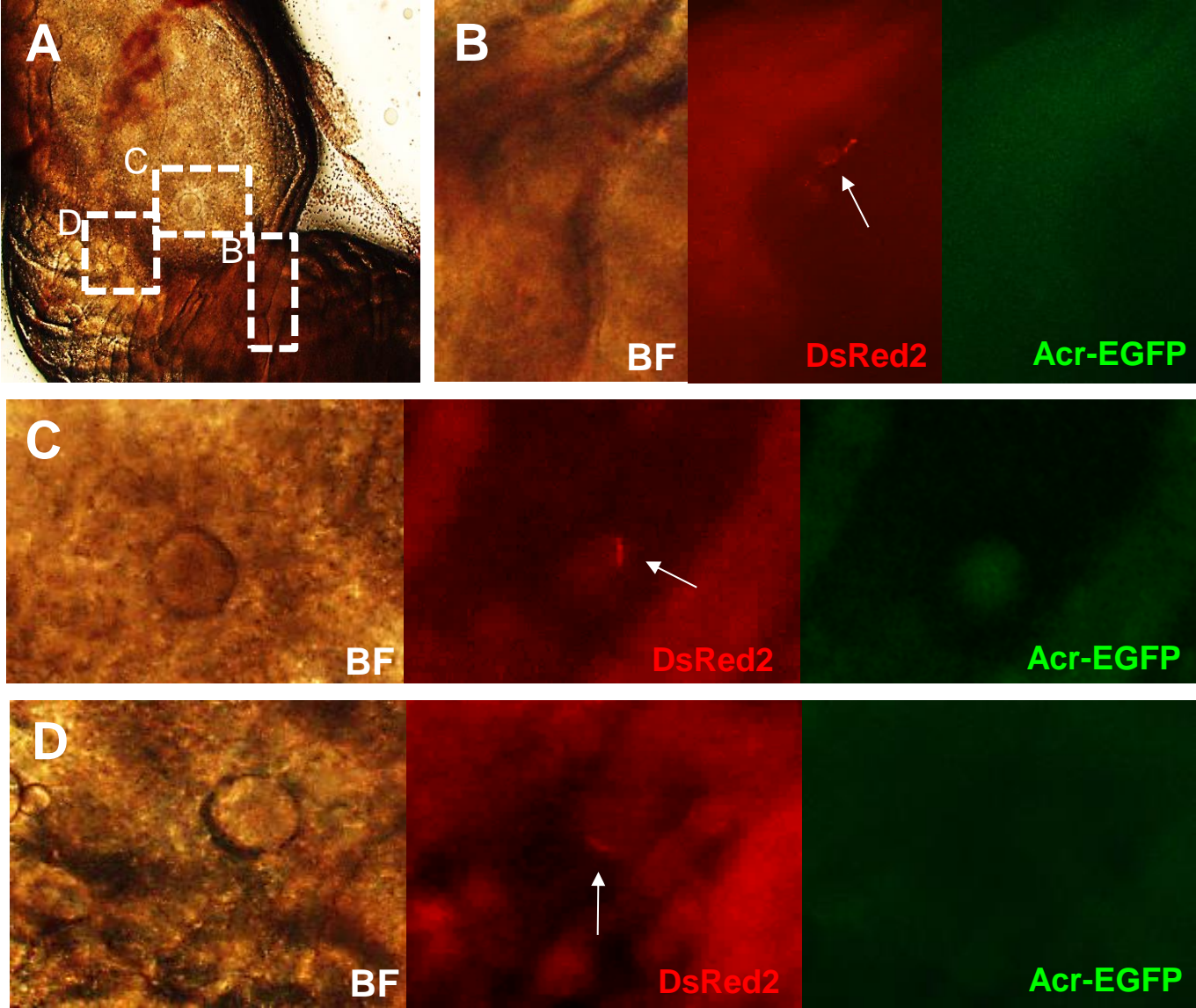


Figure 8

